Geomechanics and Engineering, *Vol. 26, No. 1 (2021) 77-88*
https://doi.org/10.12989/gae.2021.26.1.077

Experimental and numerical study on behavior of retaining structure with limited soil

Hongliu Jin[1a], Ga Zhang*[1] and Yusheng Yang[2b]

[1]*State Key Laboratory of Hydroscience and Engineering, Tsinghua University, Beijing 100084, PR China*
[2]*China Institute of Water Resources and Hydropower Research, Beijing 100084, PR China*

(Received November 7, 2019, Revised June 24, 2021, Accepted June 25, 2021)

Abstract. With the development of city construction, the situations of foundation pit excavations adjacent to an existing structure occur more frequently. A series of centrifuge model tests and numerical analyses considering actual excavation process were performed to study the deformation and earth pressure of retaining wall, deformation characteristics of retained soil with various limited soil widths. The horizontal displacement and bending moment of the retaining wall decrease with decreasing limited soil width while the rate of the decrease increases with decreasing limited soil width. The horizontal displacement of the retained soil decreases with decreasing limited soil width while the settlement of the retained soil increases with increasing limited soil width. The deformation zone is almost triangular for unlimited condition and trapezoidal for limited condition. As the limited soil width decreases, the deformation zone shrinks and the inclination of deformation zone increases. The lateral earth pressure on the retaining wall shows two-segment distribution and decreases with decreasing limited soil width. The vertical earth pressure shows non-uniform distribution along width and decreases with decreasing limited soil width due to increasing arching effect. The critical width is much smaller than excavation influence width. This may be explained by the fact that only the deformation of soil within critical width will influence the soil near the wall.

Keywords: centrifuge model test; earth pressure; foundation pit excavation; limited soil width; numerical analysis; retaining wall

1. Introduction

With the development of city construction, the density of underground engineering keeps increasing. The situations of foundation pit excavations adjacent to an existing structure occur more frequently. The soil behind the retaining structure is too narrow to fully develop the failure surface in these situations, termed limited soil. Besides, the soil between double-row piles and the backfill in narrow mine stopes or MSE (mechanical stabilized earth) walls also belong to limited soil (Hossain *et al*. 2012, Shen *et al*. 2017). In these cases, the conventional methods based on semi-infinite space assumption are no longer appropriate to estimate the failure surface and earth pressure (Coulomb 1776, Rankine 1857, Paik and Salgado 2003, Peng and Chen 2013, Altunbas *et al*. 2017, Gezgin and Cinicioglu 2019, Zhang *et al*. 2019). Given the security and economy of the project, it is necessary to understand the earth pressure for limited soil, guiding engineering design.

The study of limited soil pressure originated from investigating the pressure on the silos side wall filled with granular materials (Janssen 1895, Blight 1986, Jarrett *et al*. 1995). Janssen (1895) proposed an arching theory to describe the reduction in vertical pressure in the silos, and then Spangler and Handy (1984) applied Janssen's theory for an equation to estimate the lateral pressure on the retaining wall for backfill with an arbitrary width. The earth pressure coefficient was improved to consider principal stress deflection and wall movement (Handy 1985, Frydman and Keissar 1987, Harrop-Williams 1989, Jaouhar *et al*. 2018).

Besides, a few numerical analyses have been conducted on the retaining structures with limited soil space. Yang and Liu (2007), used the finite element software Plaxis to analyze the earth pressure in narrow MSE wall in front of stable face. Fan and Fang (2010) used Plaxis to analyze the active earth pressure distribution on rigid retaining wall near inclined rock face, which is difficult to solve analytically. In addition, the finite difference code FLAC^{2D} and FLAC^{3D} were also widely used to analyze various structures (Zucca and Valente 2020), including the limited soil contained between vertical walls (Pirapakaran and Sivakugan 2007, Sivakugan and Widisinghe 2013, Li and Aubertin 2015). Numerical analyses are economical and powerful in studying the earth pressure for limited soil, but their validity depends highly on the effectiveness of constitutive relationship and input parameters.

Physical model test is an effective method to study the earth pressure on the retaining walls with limited soil. A few 1-g model tests were conduct to investigate the earth pressure on rigid retaining walls, as well as the effect of wall aspect ratio (Fang and Ishibashi 1986, Khosravi et al. 2013), nevertheless, they are unable to reproduce the actual

*Corresponding author, Professor, Ph.D.
E-mail: zhangga@tsinghua.edu.cn
[a]Ph.D. Student
[b]Professor, Ph.D.

ISSN: 2005-307X (Print), 2092-6219 (Online)

stress state of the prototype. Centrifuge model tests can simulate the actual gravity field by increasing centrifugal acceleration, and thus reproduce stress path and deformation of the prototype in models. Frydman and Keissar (1987) conducted a series of centrifuge model tests to investigate the earth pressure on retaining walls near rock faces from at-rest to active conditions with wall rotation about base. The arching equation proposed by Spangler and Handy (1984) was validated to give a good estimation under at-rest condition but an underestimation under active condition. Take and Valsangkar (2001) performed centrifuge model tests to study the effect of backfill width on static earth pressure on unyielding retaining walls. The test results showed that the backfill width had dominant effect on the reduction of earth pressure within the narrow backfill.

The earth pressure for limited soil has been preliminarily studied considering some specific modes of rigid retaining wall, and the actual excavation process has not be well considered. In addition, there are few studies on deformation and failure characteristics of limited soil, interaction between limited soil and retaining wall and influence rules of limited soil width, though those issues are essential for a reasonable design of such types of retaining structures. In this research, a series of centrifuge model tests and numerical analyses considering actual excavation process were performed to study the behaviors and earth pressure of retaining wall, deformation characteristics of retained soil, and distribution and the influence rules of limited soil width.

2. Centrifuge model tests

2.1 Devices

The centrifuge model tests were conducted with the geotechnical centrifuge at Tsinghua University, whose effective radius is 2 m and maximum centrifugal acceleration is 250 g. The excavation of foundation pit is realized with the true stress paths in-flight using a specially developed device (Zhang and Yan 2016). The excavation device was fixed on a model container, which is made of aluminium and 60 cm long, 20 cm width, 55 cm high. One side of the model container was equipped with a piece of transparent thick polymethyl methacrylate for observation of the model during tests.

The device consists of a horizontal supporting unit and a vertical loading unit to replace the excavated soil with the compensation of its effect on the model before excavation (Fig. 1). The horizontal supporting unit is used to ensure the confining state of the retained soil, and the vertical loading unit is used to simulate the vertical gravity stress of the excavated soil on the soil base. Thus, the stress field in the soil base before excavation is considered to be equal to the soil base without removing the excavated soil. The supporting plate and the lead sheets are simultaneously removed using a remote control unit to simulate the excavation during the test.

A piece of aluminium plate, termed fixed wall in this paper, was supplemented to simulate the existing structure and change the width of retained soil (Fig. 1). The fixed wall was placed vertically at the bottom and fixed with the model container by four bolts to make it a new side wall of the model container. The width of the retained soil was changed by adjusting the length of the bolts between the fixed wall and the model container to carry out the test schemes.

2.2 Schemes and models

Four centrifuge model tests were conducted to consider various soil widths behind the retaining walls, 29 cm, 12 cm, 9 cm and 6 cm. For all the tests, the buried depth of the retaining wall was 16 cm and the excavation depth was 26 cm (Fig. 1). The 29-cm-width was sufficient for the deformation and failure of the soil due to excavation and could be regarded as unlimited condition.

The soil used in the tests was air-dried Fujian standard sand. The dry density and relative density of the soil were 1.6 g/cm^3 and 73%, relatively. The specific gravity, maximum void ratio, minimum void ratio and oedometric modulus of the soil were 2.68, 0.971, 0.567 and 51 MPa, respectively. The uniformity coefficient and average particle diameter of the soil were 2.1 and 0.19 mm, respectively. The internal friction angle of the soil and the interface friction angle between soil and aluminum measured by a series of direct shear tests were 36º and 23º, respectively.

The soil bed was prepared by the air pluviation method using an adjustable-height hopper. To attain a uniform soil base at relative density of 73%, the pouring height was kept constant at 70 cm during the sample preparation. A thin white sand layer with thickness of 0.5 cm was poured on each 1.5 cm layer of standard sand to increase the gray-level difference for image-based displacement measurement (Fig.1a).

The retaining wall was made of aluminium alloy with a width of 20 cm and a thickness of 1 cm. The wall was insert in the soil base to a depth of 42 cm. Then the excavated soil was removed and the excavation simulation device was installed to the model container. The supporting plate was adjust to contact with the retaining wall, and the lead sheets, whose mass is determined according to that of the excavated soil, was placed on the surface of the soil base.

2.3 Measurements

Fourteen pairs of strain gauges were pasted to both sides of the retaining wall along its central axis to record the strain histories during the tests, the positioning of the strain gauges was shown in Fig. 1b. The bending moment of the retaining wall could be obtained using the measured strains according to the elasticity theory. A laser-displacement transducer with an accuracy of 0.03 mm was installed to measure the horizontal displacement at the top of the retaining wall.

The lateral side of the model was observed and recorded to a series of images using an image-capture system through the transparent polymethyl methacrylate of the model container during the tests. According to the image series, the displacement of the retaining wall and soil were determined via a correlation-based analysis (Zhang *et al.*

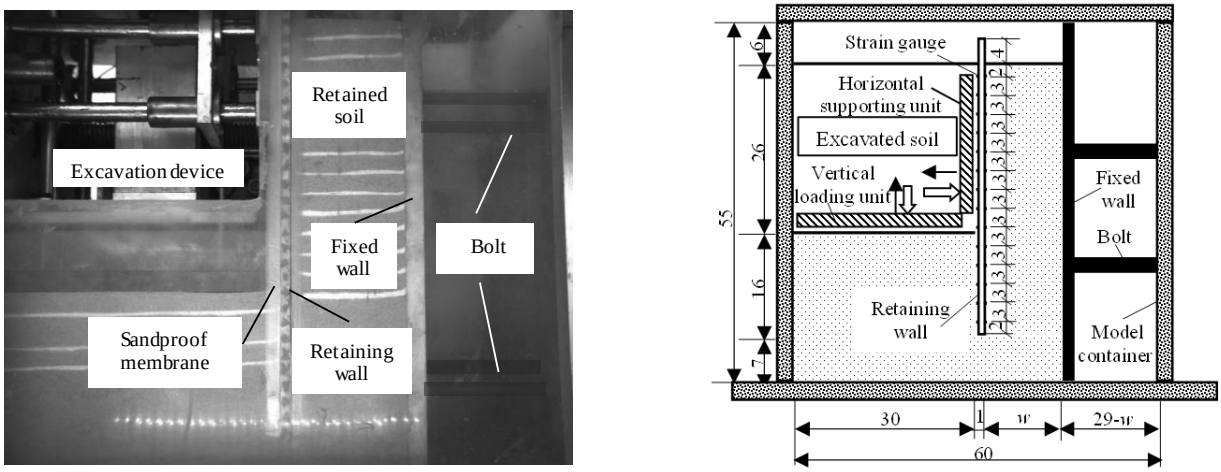

(a) Photograph (b) Elevation view

Fig. 1 Schematic view of a typical model with limited soil (unit: cm)

2009).

In this paper, all the measured results in the centrifuge model tests were presented at the model scale, which could be transformed to the prototype according to the similarity law at the 50 g level. The linear dimension such as model size and displacement could be transformed to the prototype by multiplying by 50. The bending moment could be transformed to the prototype by multiplying by 50^3. The stress and strain were equivalent for the model's and prototype's dimensions.

2.4 Process

In a centrifuge model test, the centrifugal acceleration was gradually increased to 50 g and then maintained. After the deformation of the model became steady, the excavation command was sent to the device, then the supporting plate leaved the retaining wall and the lead sheets were lifted up at the same time. The test ended if the foundation pit failed or the deformation of model became invariable. The strain of the retaining wall and the deformation of the model were recorded by strain gauges and the image capture system during tests.

3. Test observation and analysis

3.1 Response of the retaining wall

Fig. 2 compares the horizontal displacements at the top of the retaining wall in a test obtained by laser measurement and image-based measurement. It can be seen that the measurement results using different approaches agree well. This validates the accuracy of image-based measurement. Fig. 3 shows horizontal displacement distributions of the retaining wall in a test. It can be observed that the retaining wall shows a forward flexure deformation mode. The horizontal displacement is nearly zero in the lower part of the wall and exhibits a nearly linear increase with increasing elevation after the inflection. This result indicates that the retaining wall rotates towards the

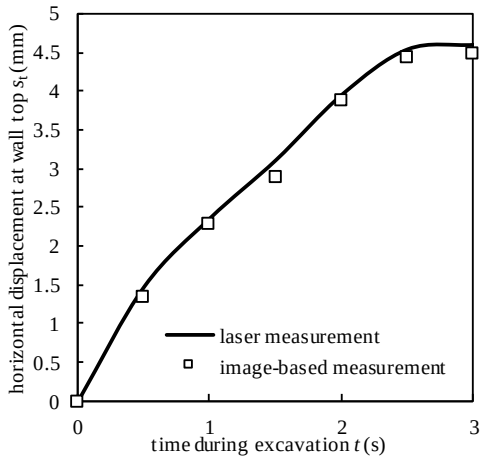

Fig. 2 History of horizontal displacement at the top of retaining wall for model with soil width of 6 cm during excavation

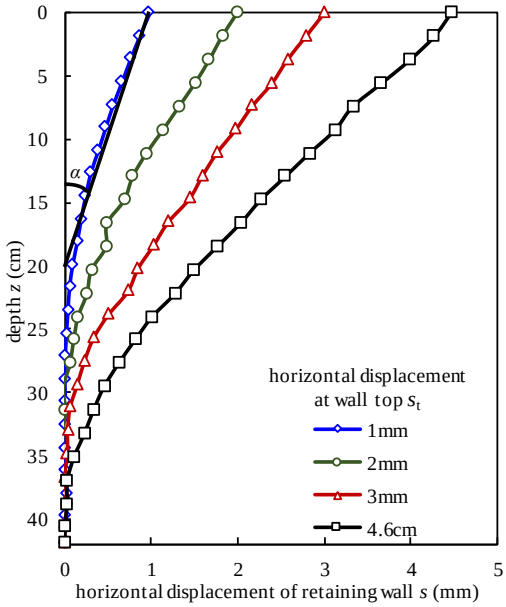

Fig. 3 Development of horizontal displacement distribution of retaining wall for model with soil width of 6 cm

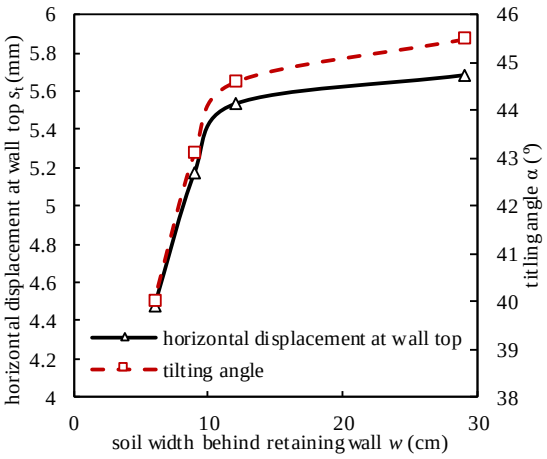

Fig. 4 Relationship between horizontal displacement at wall top and titling angle of the retaining wall and soil width

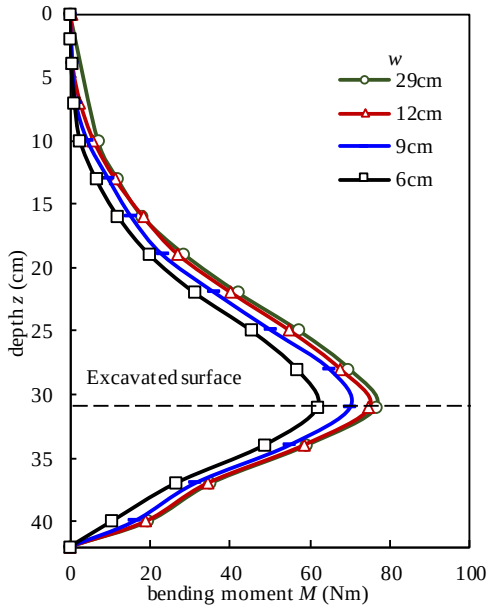

Fig. 5 Bending moment distribution of the retaining wall with various soil widths

excavation side about this inflection. Such inflection moves downward as the wall displacement increases, indicating the soil-wall interaction deepens accordingly. The inclination of the linear segment of the distribution curve is defined as the tilting angle. The tilting angle increases as the wall displacement increases. The real-time displacement of the retaining wall can be basically determined by the maximum horizontal displacement at the top and the tilting angle, which are two key parameters in evaluating the stability of such a retaining wall in engineering. Fig. 4 shows the relationship between these two indexes with soil width. It is clear that both the maximum horizontal displacement and tilting angle of the retaining wall decrease with decreasing limited soil width while the rate of the decrease increases with the decreasing limited soil width.

Fig. 5 compares the bending moment distributions of the retaining wall with various widths of retained soil. It can be observed that all curves exhibit a nearly parabolic distribution with a peak. The maximum bending moment for retaining wall with soil widths of 12 cm, 9 cm, 6 cm decreases by 1.5%, 8% and 19% respectively, compared with that of retaining wall with unlimited soil. This result indicates that the bending moment decreases with decreasing width of retained soil. Such change rule seems similar with that of the wall deflection. However, the location of the maximum bending moment is observed to be invariable and about 5 cm below the excavated surface that is not affected by the soil width.

3.2 Response of the soil

Fig. 6 shows the displacement vectors of the retained soil for different models. In all case, the significant displacements were concentrated in the upper part of the retained soil with a sliding tendency to the excavation side. The angle between the displacement vector and the vertical decreases, that is, the settlement becomes more dominating in displacement vector with decreasing limited soil width.

A detailed examination was conducted on the effect of the limited soil width on deformation magnitude according to the displacements of retained soil surface shown in Fig 7. It can be observed that the horizontal displacement decreases with increasing distance from the retaining wall. The maximum horizontal displacement decreases with the decreasing limited soil width, showing the same trend as the deflection of the retaining wall. As the boundary of the retained soil, the retaining structure has direct influence on deformation of the retained soil. In contrast to the horizontal displacement, the settlement increases with decreasing limited soil width although they are distributed more evenly. This indicates that the excavation of foundation pit with limited retained soil induces excessive settlement that will affect the surrounding structures.

Fig. 8 shows the horizontal displacement distribution at various elevations of retained soil. An inflexion can be found along the distribution curves, on the left side of which the horizontal displacement exhibits an evident increase from nearly zero, and thus it can be recognized as boundary points to distinguish the deformation zone. The flexions at various elevations, marked using dotted line in Fig. 8, were connected to determine the accurate boundary of deformation zone for the test.

Fig. 9 shows the deformation zones of the retained soil at various wall movements and the curves represent boundaries of deformation zones. It can be observed that the deformation zone is almost triangular for unlimited condition and trapezoidal for limited condition. The deformation zone firstly appears near the surface of retained soil and gradually expands as the retaining wall continues to move. It should be noted that the boundary of the deformation zone is always nearly a line with an invariable inclination. The depths of deformation zone are almost same for various soil widths at identical wall movement and close to the inflection of horizontal displacement distribution curve of retaining wall. This result confirm the fact again that the retaining structure has a direct influence on deformation of the retained soil. Fig. 10 shows the relationship between final deformation zone and soil width. It can be observed that the depth of deformation zone

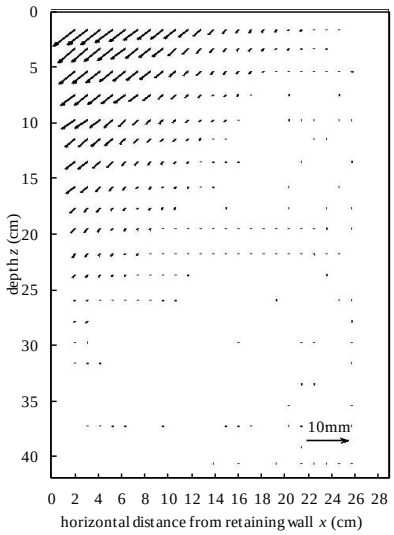

(a) w= 29 cm

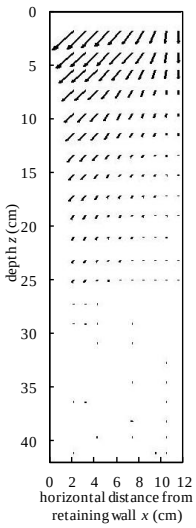

(b) w= 12 cm

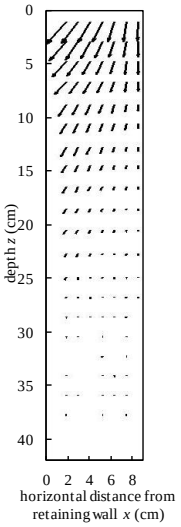

(c) w= 9 cm

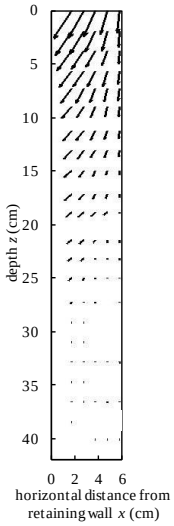

(d) w= 6 cm

Fig. 6 Displacement vectors of the retained soil for models with various soil widths, w

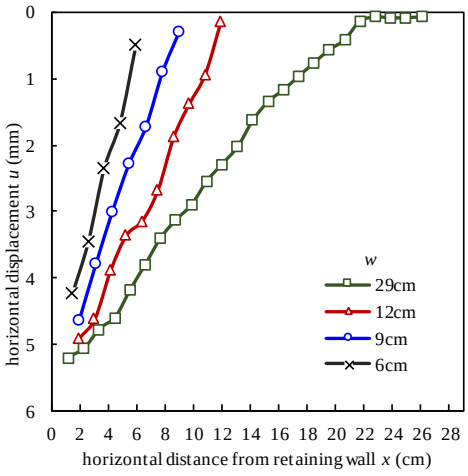

(a) Horizontal displacement

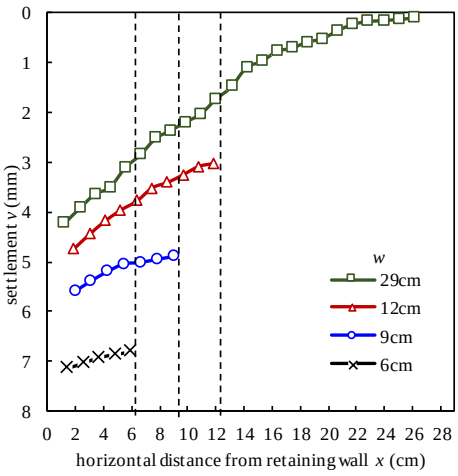

(b) Settlement

Fig. 7 Displacements of retained soil surface for models with various soil widths, w

decreases and the inclination of deformation zone increases as the limited soil width decreases (Fig. 10).

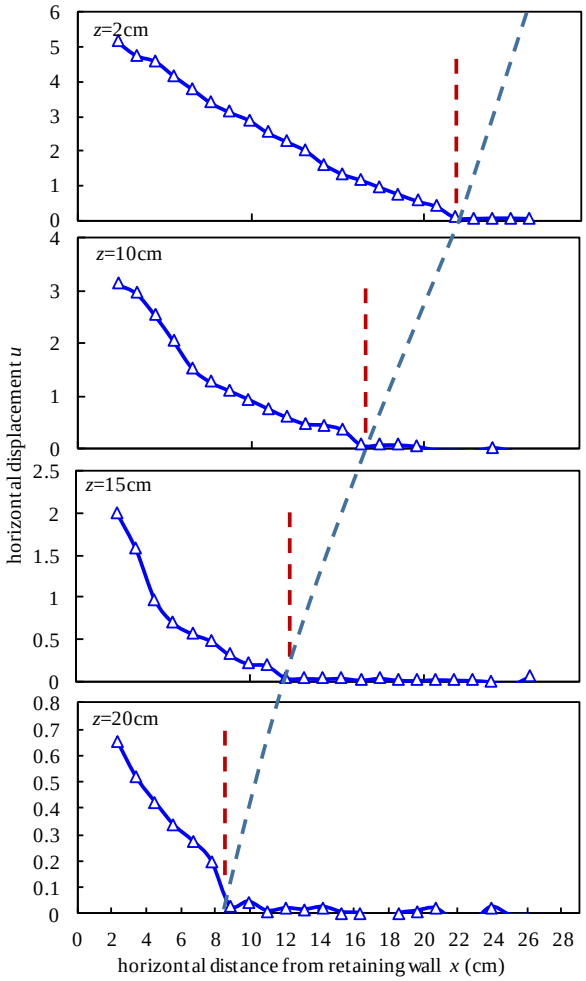

Fig. 8 Horizontal displacement distribution at various elevations of the retained soil for model with soil width of 29cm

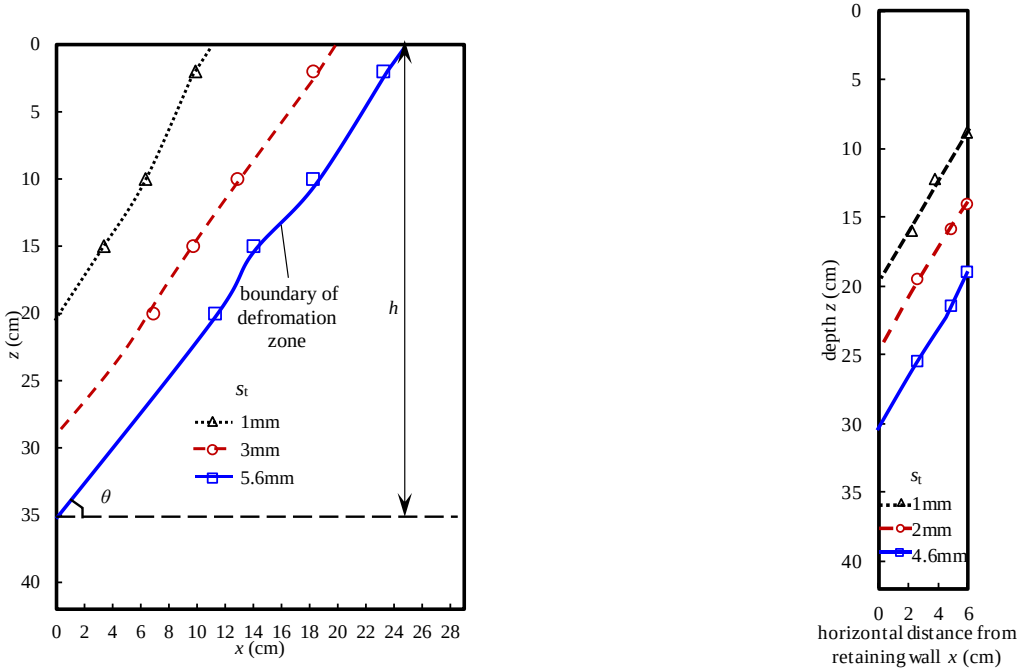

(a) Soil width behind retaining wall w= 29 cm (b) Soil width behind retaining wall w= 6 cm

Fig. 9 Deformation zones of the retained soil at various wall movements at the top, s_t

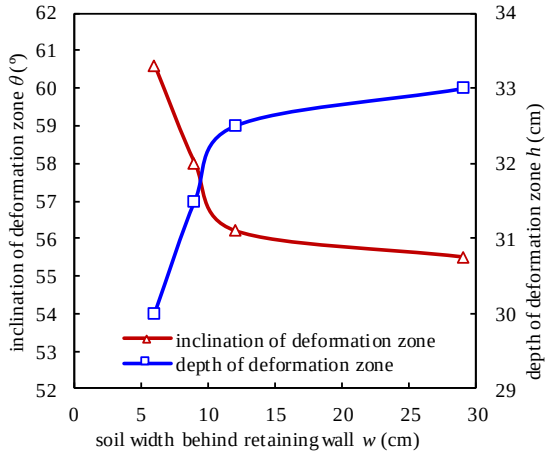

Fig. 10 Relationship between final deformation zone and soil width

4. Numerical methods

A finite element analysis was conducted on the model in centrifuge tests to obtain the stress in retained soil that could not be accurately measured in the tests.

4.1 Numerical model

A large-scale finite element software ABAQUS was used to setup two-dimensional plane strain numerical models based on the centrifuge model tests. Fig. 11 shows a typical finite element model simulating the centrifuge model test. The finite element mesh is composed of 4-node bilinear plane strain quadrilateral solid elements (CPE4 element). The Mohr-Coulomb model is used to describe behavior of the soil. The Young's modulus, Poisson's ration and dilatancy angle of the soil are empirically set to 40 MPa, 0.3 and 10º, respectively. The linear elastic model is used to model the stress-strain behavior of the retaining wall. The Young's modulus and Poisson's ration of the retaining wall are 72GPa and 0.33, respectively. The wall-soil interface is simulated using a hard contact in the normal direction and a friction model in the tangential direction. The friction coefficient is 0.424 according to the friction angle of the interface between the soil and aluminium alloy. The fixed wall on the right is set to rigid and immobile. The left side boundary was restrained in the horizontal direction, and the bottom boundary was constrained in all directions.
The finite element analysis was carried out in a few steps. The first step was applying gravity to the model without the retaining wall and the excavation. The acceleration of gravity was gradually increased to 490 m/s2 to simulate the 50 g level in the centrifuge model test. The retaining wall in the soil was then activated, and the excavated soil was finally removed via deactivation.

4.2 Validation

The numerical analysis results were compared with the centrifuge model test results (Figs. 12-14). It can be observed in Fig. 12 that the horizontal displacement of the retaining wall predicted by the numerical analysis agrees

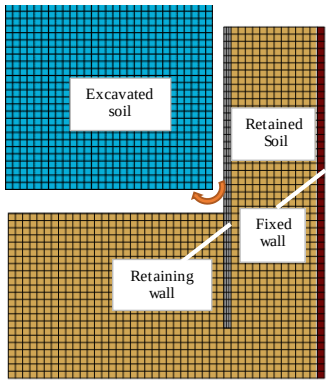

Fig. 11 The finite element mesh for a retaining wall with limited soil

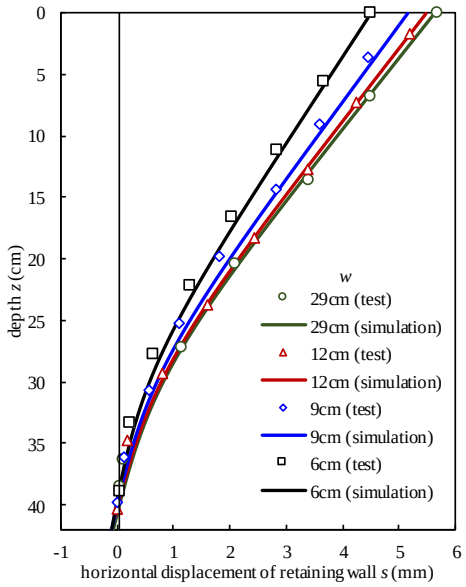

Fig. 12 Distribution of horizontal displacement of retaining wall obtained from numerical analysis and centrifuge model test. *w*, soil width behind retaining wall

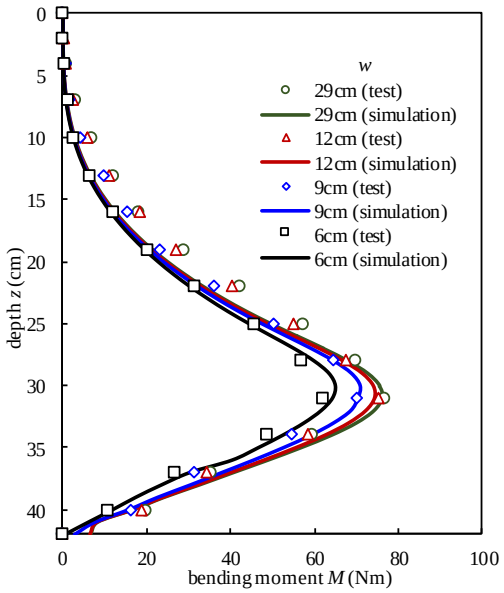

Fig. 13 Distribution of bending moment of retaining wall obtained from numerical analysis and centrifuge model test. *w*, soil width behind retaining wall

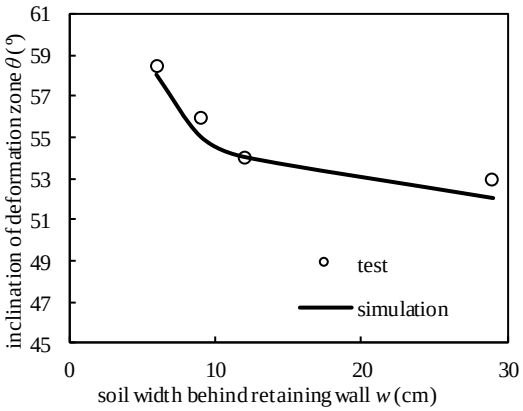

Fig. 14 Relationship between inclination of deformation zone and soil width obtained from the numerical analysis and centrifuge model tests

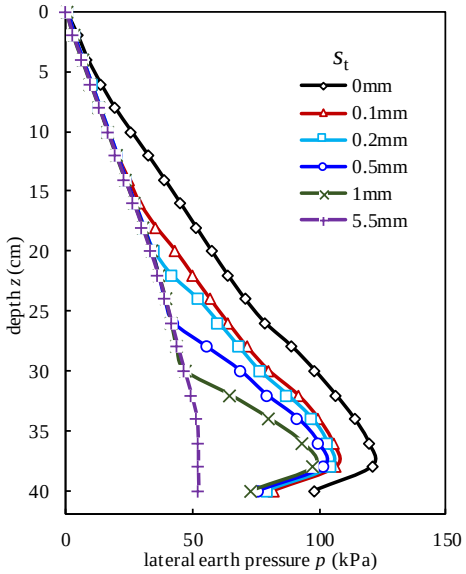

Fig. 15 Lateral earth pressure distribution at various wall movement for the model with soil width of 12 cm. s_t, horizontal displacement at wall top

well with the test observation. The horizontal displacement almost increased linearly with increasing elevation in the upper part of the wall and the maximum displacement decreased with decreasing limited soil width. The bending moment obtained from numerical analysis are close to the test measurement (Fig. 13). In addition to the response of the retaining wall, the response of the soil also obtained good agreement. The relationship between inclination of deformation zone and soil width obtained from numerical analysis and test observation were compared to be consistent (Fig. 14).

In conclusion, the numerical models were confirmed to be effective to simulate the response of the soil-retaining wall system in centrifuge model tests and could be used for further analysis.

5. Numerical result and analysis

5.1 Lateral earth pressure analysis

The lateral earth pressure along the retaining wall at various wall movement for the model with the soil width of 12 cm is shown in Fig. 15. It can be observed that the earth pressure at an elevation decreases with increasing wall movement and then eventually becomes nearly invariable. All distribution curves have the same shape at various wall movement and can be divided into two segments by an inflection, which descents as the wall moves. The lateral earth pressure above this flection becomes invariable and decrease with increasing wall movement below the flection. Since the horizontal displacement of the retaining wall is strictly controlled in practice, Fig. 16a compares the lateral earth pressure against the retaining wall with various soil widths at horizontal displacement at wall top of 1mm. The earth pressure according to the Coulomb's active earth pressure theory is also plotted in the figure for reference. As shown in the figure, the lateral earth pressure on the retaining wall decreases with decreasing limited soil width whether it becomes invariable for identical wall movement. Whereas, the location of the inflection of the lateral earth pressure is almost same and not affected by the soil width for identical wall movement.

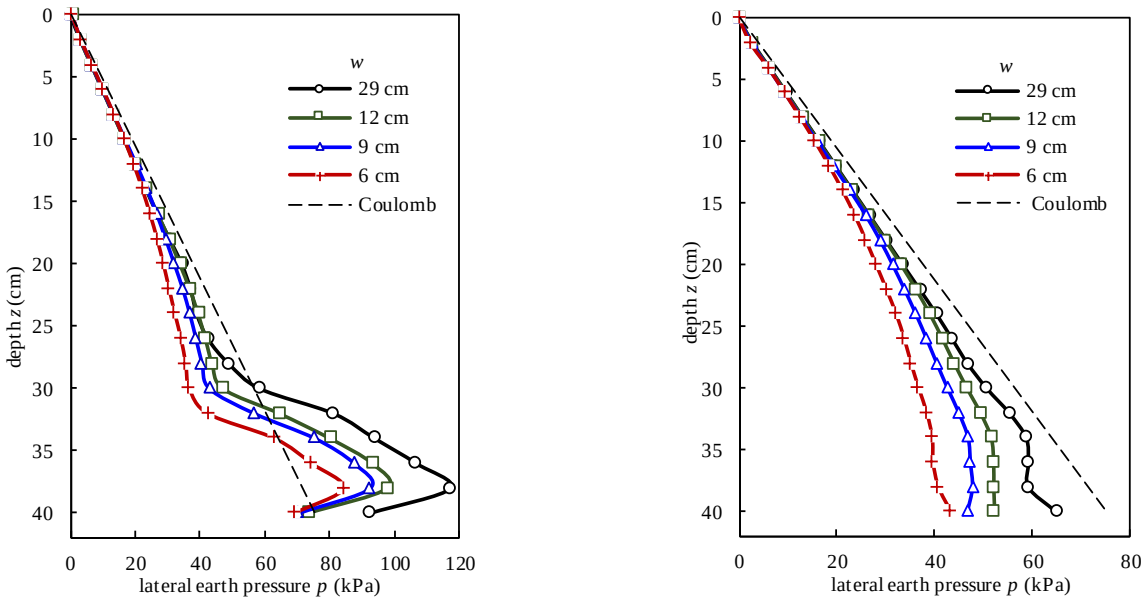

(a) Horizontal displacement at wall top s_t =1 mm (b) At the end of the tests

Fig. 16 Horizontal earth pressures distribution for models with various soil widths. *w*, soil width behind wall

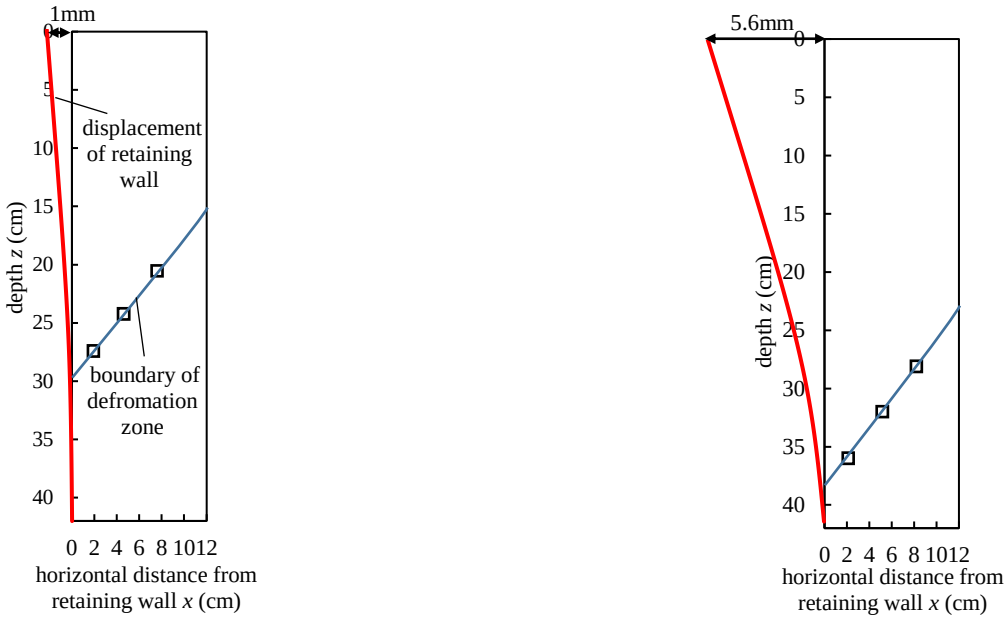

(a) Horizontal displacement at wall top s_t =1 mm (b) At the end of the tests

Fig. 17 Deformation zones of retained soil and horizontal displacement distributions of retaining wall for the model with soil width of 12 cm at different times from numerical analysis

Fig. 16(b) shows the lateral earth pressure for various soil width at the end of the tests. Besides the discrepancy at z >36 cm for test at soil width of 6 cm, the lateral earth pressure along the retaining wall at various elevations for all tests reached constant values before the end of the tests. It can be found that the lateral earth pressure increases nearly linearly with increasing depth for unlimited condition while increases logarithmically with increasing depth and tends to an asymptotic values for limited condition. The final earth pressure decreases with decreasing soil width while the rate of the decrease increases with decreasing limited soil width. This result can explain why the horizontal displacement and the bending moment of the retaining wall at the end of the tests decrease exponentially with the decreasing soil width. Besides, it can be found as well in Fig. 16(b) that the differences among these distribution curves gradually increase as the depth increases.

Fig. 17 shows the deformation zones of retained soil and horizontal displacement distributions of retaining wall for the model with soil width of 12 cm at different times from numerical analysis. The deformation zone of retained soil

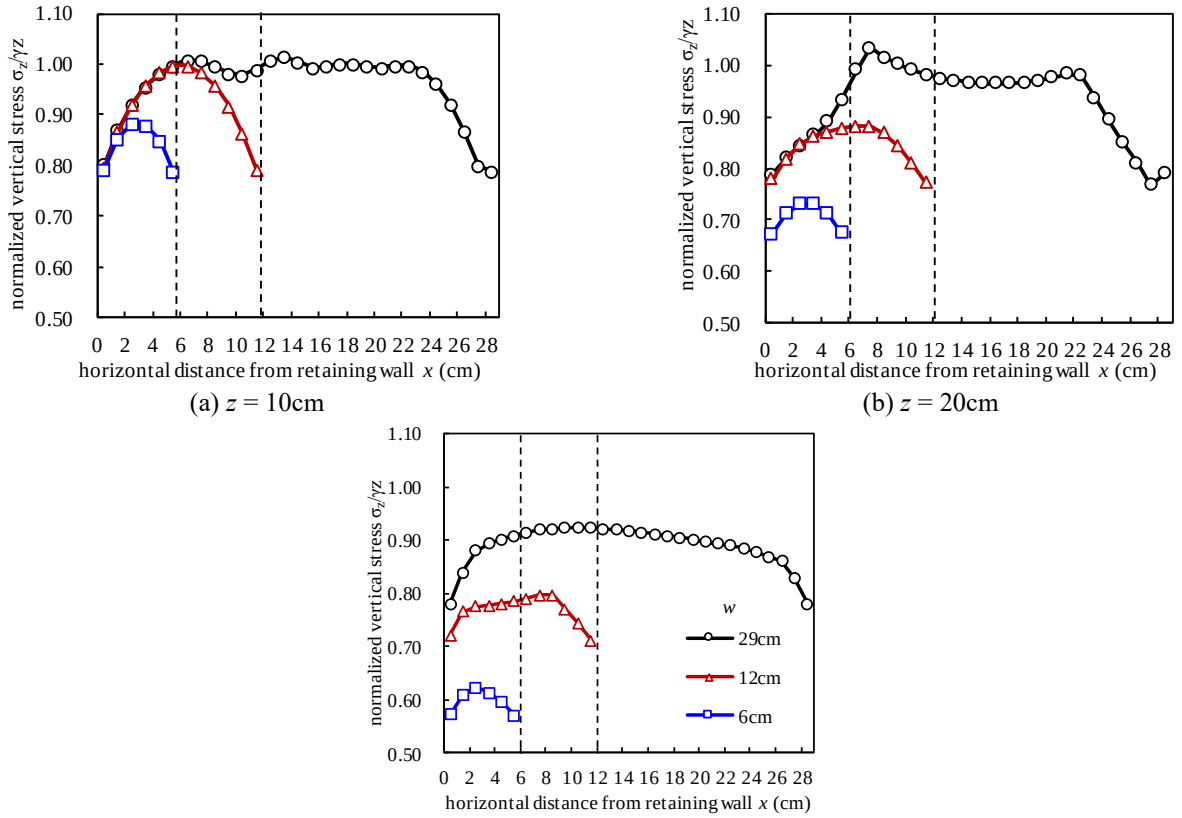

Fig. 18 Vertical stress distribution along width for models with various soil widths, w

gradually expands with wall movement and the depths of deformation zone are close to the inflection of horizontal displacement of retaining wall, which agrees well with test results. In addition, it can be found as well that the inflection of lateral earth pressure is close to the depth of deformation zone as well as the inflection of horizontal displacement of retaining wall. This indicates that the wall movement affects the development of the deformation zone of retained soil and thus affects the distribution of lateral earth pressure.

5.2 Vertical earth pressure analysis

The distribution of normalized vertical stresses of soil elements at various elevations is plotted in Fig. 18. It can be observed that vertical stress shows non-uniform distribution along width due to the arching effect and the vertical earth pressure decreases with the decreasing limited soil width. The influence of wall friction decreases with increasing distance from the walls. If soil space is wide enough to develop a complete slip surface, only one side wall friction will decrease the vertical earth pressure. If the retained soil is limited, both boundaries will mobilize wall friction. The arching effect will increase with decreasing limited soil width, and thus the vertical earth pressure decreases with the decreasing limited soil width. This fact can explain why the lateral earth pressure on the retaining wall decreases with decreasing limited soil width. In addition, it can be observed that the normalized vertical earth pressure decreases with increasing depth. This is because that the wall friction effect on the reduction in total vertical force of the soil near the wall is cumulative along depth.

6. Critical width of limited soil

As for the centrifuge model tests, it can be found from Fig. 9(a) that the excavation influence width according to the deformation zone for test models in this paper is about 22 cm (0.85 times excavation depth). Theoretically, if the soil width is less than this width, the deformation of the soil will be affected by the boundary constraint and the soil is limited. However, it can be observed from Figs. 4 and 5 that the maximum horizontal displacement and bending moment of the retaining wall decreases exponentially with decreasing limited soil width. The results for the model with soil width of 12 cm is very close to that for models with unlimited soil. For example, the difference of maximum horizontal displacement and maximum bending moment of the retaining wall between these two models are only 2% and 1.5% respectively. In the light of the actual engineering, 12 cm (0.55 times excavation influence width) can be used as the critical width within a margin of error to determine whether the retained soil is limited.

To further explore and verify the critical width of limited soil, numerical models with soil width of 15 cm, 18 cm, and 20 cm were supplemented. The excavation influence width obtained from numerical analysis is 23 cm

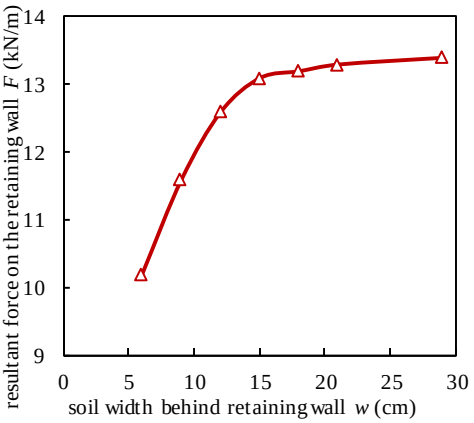

(a) Resultant force on the retaining wall

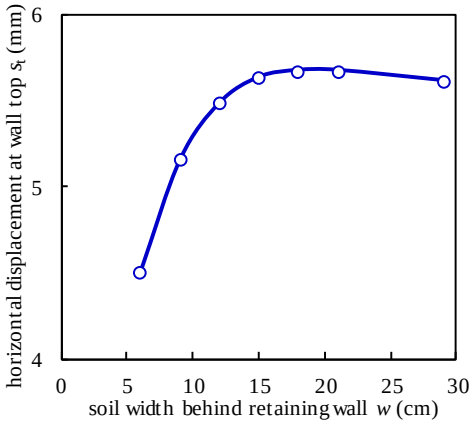

(b) Horizontal displacement at wall top

Fig. 19 Relationship between predicted results and soil width

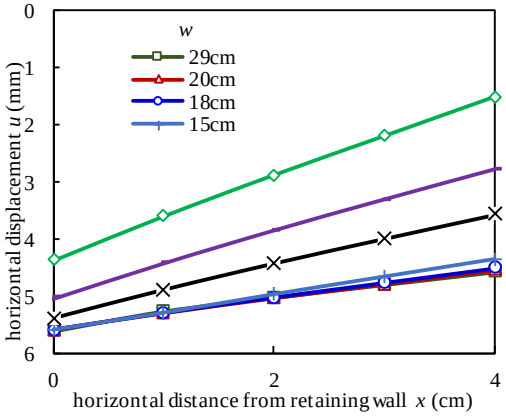

Fig. 20 Displacements of retained soil surface near the retaining wall for models with various soil widths obtained from the numerical analysis. *w*, soil width behind wall

(0.88 times excavation depth). Lateral earth pressure, wall deflection are the two most concerned topics. Fig. 19 shows the relationship between the responses and the soil width. The inflection for curves of resultant force and maximum horizontal displacement both occur at the soil width of 14 cm (0.6 times excavation influence width). The critical width of limited soil is much smaller than the excavation influence width. This result may be explained by the fact that the deformation of the soil over 14 cm away from the retaining wall has little effect on the soil near the retaining wall (Fig. 20). In other word, only the deformation of the soil within critical width will influence the soil near the wall.

The critical width is 14 cm and 0.6 times excavation influence width in this paper. However, the critical width is affected by various factors, such as excavated depth, embedded depth, wall stiffness and soil parameter, and will be systematically analyzed in future studies.

7. Conclusions

The deformation and earth pressure of flexible cantilever retaining wall and deformation characteristics of retained soil with various limited soil widths, were investigated by using centrifuge model tests and numerical analyses. The following conclusions can be drawn:

- The horizontal displacement and bending moment of the retaining wall decrease with the decreasing limited soil width while the rate of the decrease increases with the decreasing limited soil width.
- The horizontal displacement of the retained soil decreases with the decreasing limited soil width while the settlement of the retained soil increases with the decreasing limited soil width, indicating that the excavation of foundation pit with limited retained soil induces excessive settlement that will affect the surrounding structures.
- The deformation zone is almost triangular for unlimited condition and trapezoidal for limited condition. As the limited soil width decreases, the depth of deformation zone decreases and the inclination of deformation zone increases.
- The lateral earth pressure shows two-segment distribution. The wall movement affects the deformation zone of retained soil and thus affects the distribution of lateral earth pressure. The lateral earth pressure on the retaining wall decreases with decreasing limited soil width, explaining why the horizontal displacement and the bending moment of the retaining wall decrease exponentially with the decreasing soil width.
- The vertical earth pressure shows non-uniform distribution along width due to the arching effect. The arching effect will increase with decreasing limited soil width and thus the vertical earth pressure decreases with the decreasing limited soil width.
- The critical width of limited soil is much smaller than the excavation influence width. This may be explained by the fact that only the deformation of soil within critical width will influence the soil near the wall.

Acknowledgments

The study is supported by Open Research Fund Program

of State key Laboratory of Hydroscience and Engineering (sklhse-2021-D-04), Tsinghua University Initiative Scientific Research Program, and National Natural Science Foundation of China (52039005).

References

Altunbas, A., Soltanbeigi, B. and Cinicioglu, O. (2017), "Determination of active failure surface geometry for cohesionless backfills", *Geomech. Eng.*, **12**(6), 983-1001. https://doi.org/10.12989/gae.2017.12.6.983.

Blight, G.E. (1986), "Pressure exerted by materials stored in silos: Part I, coarse materials", *Geotechnique*, **36**(1), 33-46. https://doi.org/10.1680/geot.1986.36.1.33.

Coulomb, C.A. (1776), "An attempt to apply the rules of maxima and minima to several problems of stability related to architecture", *Mem. Acad. Roy. des Science*, 7, 343-382.

Fan, C.C. and Fang, Y.S. (2010), "Numerical solution of active earth pressures on rigid retaining walls built near rock faces", *Comput. Geotech.*, **37**, 1023-1029. https://doi.org/10.1016/j.compgeo.2010.08.004.

Fang, Y.S. and Ishibashi, I. (1986), "Static earth pressures with various wall movements", *J. Geotech. Eng.*, **112**(3), 317-333. https://doi.org/10.1061/(ASCE)0733-9410(1986)112:3(317).

Frydman, S.F. and Keissar, I. (1987), "Earth pressure on retaining walls near rock faces", *J. Geotech. Eng.*, **113**(6), 586-599. https://doi.org/10.1061/(ASCE)0733-9410(1986)112:3(317).

Gezgin, A.T. and Cinicioglu, O. (2019), "Consideration of locked-in stresses during backfill preparation", *Geomech. Eng.*, **18**(3), 247-258. https://doi.org/10.12989/gae.2019.18.3.247.

Handy, R.L. (1985), "The arch in soil arching", *J. Geotech. Eng.*, **111**(3), 302-318. https://doi.org/10.1061/(ASCE)0733-9410(1985)111:3(302).

Harrop-Williams, K.O. (1989), "Geostatic wall pressures", *J. Geotech. Eng.*, **115**(9), 1321-1325. https://doi.org/10.1061/(ASCE)0733-9410(1989)115:9(1321).

Hossain, M.S., Kibria, G., Khan, M.S., Hossain, J. and Taufiq, T. (2012), "Effect of backfill soil on excessive movement of MSE wall", *J. Perform. Constr. Fac.*, **26**(6), 793-802. https://doi.org/10.1061/(ASCE)CF.1943-5509.0000281.

Janssen, H.A. (1895), "Versuche uber getreideedruck in silozellen", *Z. Ver. Dtsch. Ing.*, **39**, 1045-1049.

Jaouhar, E.M., Li, L., and Aubertin, M. (2018), "An analytical solution for estimating the stresses in vertical backfilled stopes based on a circular arc distribution", *Geomech. Eng.*, **15**(3), 889-898. https://doi.org/10.12989/gae.2018.15.3.889.

Jarrett, N.D., Brown, C.J. and Moore, D.B. (1995), "Pressure measurements in a rectangular silo", *Geotechnique*, **45**(1), 95-104. https://doi.org/10.1680/geot.1995.45.1.95.

Khosravi, M.H., Pipatpongsa, T. and Takemura, J. (2013), "Experimental analysis of earth pressure against rigid retaining walls under translation mode", *Geotechnique*, **63**(12), 1020-1028. https://doi.org/10.1680/geot.12.P.021.

Li, L. and Aubertin, M. (2015), "Numerical analysis of the stress distribution in symmetrical backfilled trenches with inclined walls", *Ind. Geotech. J.*, **45**(3), 278-290. https://doi.org/10.1007/s40098-014-0131-5.

Paik, K.H. and Salgado, R. (2003), "Estimation of active earth pressure against rigid retaining walls considering arching effects", *Geotechnique*, **53**(7), 643-653. https://doi.org/10.1680/geot.2003.53.7.643.

Peng, M.X. and Chen, J. (2013), "Slip-line solution to active earth pressure on retaining walls", *Geotechnique*, **63**(12), 1008-1019. https://doi.org/10.1680/geot.11.P.135.

Pirapakaran, K., and Sivakugan, N. (2007), "Arching within hydraulic fill stopes", *Geotech. Geol. Eng.*, **25**(1), 25-35. https://doi.org/10.1007/s10706-006-0003-6.

Rankine, W.J.M. (1857), "On the stability of loose earth", *Philos. T. Royal Soc. London*, **147**, 9-27. https://doi.org/10.1098/rstl.1857.0003.

Shen, Y.J., Wu, Z.J., Xiang, Z.L., Yang, M. (2017), "Physical test study on double-row long-short composite anti-sliding piles", *Geomech. Eng.*, **13**(4), 621-640. https://doi.org/10.12989/gae.2017.13.4.621.

Sivakugan, N. and Widisinghe, S. (2013), "Stresses within granular materials contained between vertical walls", *Ind. Geotech. J.*, **43**(1), 30-38. https://doi.org/10.1007/s40098-012-0029-z.

Spangler, M.G., Handy, R.L (1984), *Soil Engineering*, Harperand Row, New York, U.S.A.

Take, W.A., and Valsangkar, A.J. (2001), "Earth pressures on unyielding retaining walls of narrow backfill width", *Can. Geotech. J.*, **38**(6), 1220-1230. https://doi.org/10.1139/t01-063.

Yang, K.H., and Liu, C.A. (2007), "Finite element analysis of earth pressures for narrow retaining walls", *J. GeoEng.*, **2**(2), 43-52.

Zhang, D.B., Jiang, Y. and Yang, X.L. (2019), "Estimation of 3D active earth pressure under nonlinear strength condition", *Geomech. Eng.*, **17**(6), 515-525. https://doi.org/10.12989/gae.2019.17.6.515.

Zhang, G., Hu, Y. and Zhang, J.M. (2009), "New image analysis-based displacement-measurement system for geotechnical centrifuge modeling tests", *Measurement*, **42**(1), 87-96.

Zhang, G. and Yan, G.C. (2016), "In-flight simulation of the excavation of foundation pit in centrifuge model tests", *Geotech. Testing. J.*, **39**(1), 59-68.

Zucca, M. and Valente, M. (2020), "On the limitations of decoupled approach for the seismic behaviour evaluation of shallow multi-propped underground structures embedded in granular soils", *Eng. Struct.*, **211**, 1-15. https://doi.org/10.1016/j.engstruct.2020.110497.

CC